The transcription factor *Tfap2e*/AP-2ε plays a pivotal role in maintaining the identity of basal vomeronasal sensory neurons

Jennifer M. Lin[1], Ed Zandro M. Taroc[1], Jesus A. Frias[1], Aparna Prasad[1], Allison N. Catizone[1], Morgan A. Sammons[1] and Paolo E. Forni[1]*

[1]Department of Biological Sciences, University at Albany, Albany, NY 12222, USA.

*Author for correspondence (pforni@albany.edu)

Highlights

- The VNO contains two major cell types that are segregated in apical and basal regions of the VNO
- AP-2ε is expressed in postmitotic basal vomeronasal sensory neurons.
- AP-2ε is essential to maintain the identity of basal vomeronasal sensory neurons.

ABSTRACT

The identity of individual neuronal cell types is defined by the expression of specific combinations of transcriptional regulators that control cell type–specific genetic programs. The epithelium of the vomeronasal organ of mice contains two major types of vomeronasal sensory neurons (VSNs): 1) the apical VSNs which express vomeronasal 1 receptors (V1r) and the G-protein subunit Gαi2 and; 2) the basal VSNs which express vomeronasal 2 receptors (V2r) and the G-protein subunit Gαo. Both cell types originate from a common pool of progenitors and eventually acquire apical or basal identity through largely unknown mechanisms.

The transcription factor AP-2ε, encoded by the *Tfap2e* gene, plays a role in controlling the development of GABAergic interneurons in the main and accessory olfactory bulb (AOB), moreover AP-2ε has been previously described to be expressed in the VSNs.

Here we show that AP-2ε is expressed in postmitotic VSNs after they commit to the basal differentiation program. Loss of AP-2ε function resulted in reduced number of basal VSNs and in an increased number of neurons expressing markers of the apical lineage. Our

work suggests that AP-2ε, which is expressed in late phases of differentiation, is not needed to initiate the apical-basal differentiation dichotomy but for maintaining the basal VSNs' identity by preventing the expression of apical genes. Moreover, our data suggest that differentiated VSNs of mice retain a notable level of plasticity.

INTRODUCTION

The vomeronasal organ (VNO) is an olfactory sub-system of vertebrates specialized for the detection of pheromones. Each vomeronasal sensory neuron (VSN) selectively expresses only one or two vomeronasal receptors (VR) out of hundreds encoded by the V1r or V2r gene superfamilies (Silvotti et al., 2007), and are regenerated throughout life (Brann and Firestein, 2010; Giacobini et al., 2000; Oboti et al., 2015).

Neurons located within the apical region of the vomeronasal epithelium (VNE) express V1rs (Dulac and Axel 1995), the Gα-protein subunit Gαi2, the transcription factor (TF) Meis2 (Enomoto et al., 2011), and project to the anterior accessory olfactory bulb (AOB). VSNs distributed in the basal regions of the VNE, express V2Rs, Gαo, and project to the posterior AOB (Montani et al., 2013; Tirindelli and Ryba, 1996).

A common pool of Ascl-1+ neural progenitor cells (NPCs) resides at the lateral and basal margins of the VNE and generates neuronal precursors which differentiate into apical or basal VSNs (Cau et al., 1997; de la Rosa-Prieto et al., 2010; Martinez-Marcos et al., 2000; Murray et al., 2003). Although significant progress has been made in understanding the molecular basis of chemosensory detection, little information exists on how the terminal differentiation of apical and basal VSNs is established and cellular plasticity is restricted (Enomoto et al., 2011; Oboti et al., 2015).

The identity of specific neuronal cell types is defined and maintained by the sets of transcriptional regulators that control type–specific genetic programs (Hobert, 2016; Patel and Hobert, 2017). Bcl11b/Ctip2 is currently the only TF found to play a role in controlling VSN differentiation, as a permissive factor for the basal VSN program, as Bcl11b null mutants display a significant loss of immature basal neurons, increase of immature apical neurons, however an overall decrease in VSNs that reach maturity (Enomoto et al., 2011). Moreover, Bcl11b nulls do not survive postnatally, limiting long-term analysis of defective differentiation on the VNE and AOB morphology and function. Microarray data from

Bcl11b null mutants identified reduced expression of *Tfap2e* (AP-2ε), which has since been proposed as a potential player in directing the apical-basal dichotomy in the VNO (Suarez, 2011), although never experimentally tested.

In this work, we exploited an AP-2ε null mouse line (Feng et al., 2009), where a Cre recombinase gene has been inserted into the endogenous AP-2ε genomic locus. Unlike Bcl11b null mice, AP-2ε nulls are viable with no gross structural abnormalities. We used this mouse line to determine the impact of AP-2ε loss-of-function on VSN terminal differentiation and circuit formation in the AOB at postnatal stages by following AP-2ε expression and genetic lineage.

We established that, in the accessory olfactory system, AP-2ε is expressed by postmitotic neurons in the basal portion of the VNO and by the mitral cells of the anterior portion of the AOB. We demonstrated that AP-2ε controls the terminal differentiation and homeostasis of basal VSNs by repressing gene expression from the apical genetic program.

MATERIALS AND METHODS

Animals

The AP-2εCre line (*Tfap2e*$^{tm1(cre)Will}$) were obtained from Dr. Trevor Williams, Department of Craniofacial Biology, University of Colorado, and characterized on a Black Swiss background (Feng et al., 2009). *(Rosa)26Sor*^{Tos} (B6.129X1-*Gt(ROSA)26Sor*$^{tm1(EYFP)Cos}$/J) (termed *R26*^{YFP}) reporter mice (Srinivas et al., 2001) and R26RtdTomato (B6.Cg-Gt(ROSA)26Sortm9$^{(CAG-tdTomato)Hze}$/J) (Madisen et al., 2010) were purchased from (Jackson Laboratories, Bar Harbor, ME). Lineage tracing experiments were done on littermate mice on Black Swiss/C57F3 mixed background. Mutant and wild-type mice of either sex were used. All mouse studies were approved by the University at Albany Institutional Animal Care and Use Committee (IACUC).

Tissue Preparation

Tissue collected at ages ≥P8 were perfused with PBS then 3.7% formaldehyde in PBS. Brain tissue was isolated at the time of perfusion and additionally immersion-fixed for 3-

4 hours at 4°C. Noses were immersion fixed in 3.7% formaldehyde in PBS at 4°C overnight then decalcified in 500mM EDTA for 3-4 days. All samples were cryoprotected in 30% sucrose in PBS overnight at 4°C then embedded in O.C.T. (Tissue-TeK) using dry ice, and stored at -80°C. Tissue was cryosectioned using a CM3050S Leica cryostat at 16μm for VNOs and 20μm for OBs and collected on VWR® Superfrost® Plus Micro Slides for immunostaining and in situ hybridizations (ISH). All slides were stored at -80°C until ready for staining.

Immunohistochemistry

Citrate buffer (pH 6) microwave antigen retrieval (Forni et al., 2006) was performed, for all the antibodies indicated with asterisks (*). Primary antibodies and concentrations used in this study were, *Gt α–AP-2ε (2ug/mL, sc-131393 X, Santa Cruz, Dallas, TX) **Rt α-BrdU (1:250, NB500-169, Novus Biologicals, Littleton, CO)*Rb α–Cleaved Caspase-3 (1:1000, AB3623, Millipore, Darmstadt, Germany), *Ms α–Gαi2 (1:200, 05-1403, Millipore), Rb α–Gαo (1:1000, 551, Millipore), Rb α–GAP43 (1:500, 16053, Abcam, Cambridge, MA), Chk α–GFP (1:1000, ab13970, Abcam,), Rb α–GFP (1:2000, A-6455, Molecular Probes, Eugene, OR) *Rb α–Ki67 (1:1000, AB9260, Millipore), *Ms α–Meis2 (1:500, sc-515470, Santa Cruz), *Ms α–NeuroD1 (1:100, sc-46684, Santa Cruz), Gt α–Nrp2 (1:4000, AF567, R&D Systems, Minneapolis, MN), Gt α–OMP (1:4000, 5441001, WAKO, Osaka, Japan), *Ms α–Tbx21 (1:400, sc-21749, Santa Cruz) Rb α–V2R2 (1:4000, Gift from Dr. Roberto Tirindelli, Univ. degli Studi di Parma, Italy). Sections were pre-incubated 1.0M HCl at 37° for 30 minutes prior to anti-BrdU immunostaining (Forni et al., 2011).

For chromogen-based reactions, tissue was stained as previously described (Forni et al., 2011.). Staining was visualized with the Vectastain ABC Kit (Vector, Burlingame, CA) using diaminobenzidine (DAB) (Forni et al., 2011); sections were counterstained with methyl green.

Species-appropriate secondary antibodies conjugated with either Alexa Fluor 488, Alexa Fluor 594, Alexa Fluor 568, Alexa Fluor 680 were used for immunofluorescence detection (Molecular Probes and Jackson Laboratories, Westgrove, PA). Sections were

counterstained with 4',6'-diamidino-2-phenylindole (DAPI) (1:3000; Sigma-Aldrich) and coverslips were mounted with FluoroGel (Electron Microscopy Services). Confocal microscopy pictures were taken on a Zeiss LSM 710 microscope. Epifluorescence pictures were taken on a Leica DM4000 B LED fluorescence microscope equipped with a Leica DFC310 FX camera. Images were further analyzed using FIJI/ImageJ software.

In Situ Hybridization

Probes against transcripts derived from *Big2* and Meis2 were donated to us by Dr. J Hirota, Tokyo Institute of Technology, Japan and prepared as previously described (Enomoto et al., 2011). Plasmids to generate probes specific for Gαo and Gαi2 were provided by J.F. Cloutier, McGill University, Montreal, Canada (Cloutier et al., 2004). Briefly, digoxigenin-labeled cRNA probes were prepared by *in vitro* transcription (DIG RNA labeling kit; Roche Diagnostics). In situ hybridization was performed as described (Forni et al., 2013) and visualized by immunostaining with an alkaline phosphatase conjugated anti-DIG (1:1000), and NBT/BCIP developer solution (Roche Diagnostics).

Microarray

The whole VNOs of P17 AP-2$\varepsilon^{-/-}$ nulls and wild-type controls (n≥3 per genotype) were isolated, digested, and used to extract RNA using the PureLink™ RNA Mini Kit (Ambion by Life Technologies). RNA sample quality was tested using Agilent\2100 bioanalyzer. Whole transcriptome analysis was performed on Affymetrix Mouse Gene ST 2.0 at the Center of Functional Genomics, University at Albany, SUNY. Data analysis was performed using Transcriptome Analysis Console (TAC 4.0) Software, Applied Biosystems. Expression of selected genes of interest with significance p-value >0.05 was further validated. Microarray data was deposited in GEO (GSE110083).

qRT PCR

cDNA from Wildtype and AP-2ε null VNOs (n=3 per genotype, P15) was generated from 1,000 ng of RNA per biological replicate using the *Applied Biosystems* High Capacity cDNA kit (#4368814). Samples were amplified and measured using the *Bio-Rad iTaq Universal SYBR Green Supermix* and the *Applied Biosystems 7900HT* instrument. All

samples were run with three technical replicates and a relative standard curve was generated by serially diluting the samples. All values are relative to the standard curve and normalized to *Gapdh.* Two-tailed, unpaired t-tests were performed between wildtype and knockout mouse data. qPCR primers for each of the genes analyzed are available in Table 1.

BrdU birthdating and cell fate tracking

Intraperitoneal (IP) BrdU injections (50mg/kg) were performed on P7 control and null lineage traced mice on a mixed C57B/Black Swiss background. Samples were collected at P21 (post-injection day 14) as described in (de la Rosa-Prieto et al., 2010). Immunostainings against BrdU, tdTomato, Gαo, and Gαi2 were performed and analyzed using FIJI software. Number of BrdU+ and BrdU+/tdTomato+ cells were quantified and averaged across three series per animal. Cell counts were performed as described in *Quantification and statistical analyses of microscopy data*.

Quantification and statistical analyses of microscopy data.

Measurements of VNE and cell counts were performed on confocal images of coronal serial sections immunostained for the indicated targets. In animals ≥P15, the most central 6-8 sections on the rostro-caudal axis of the VNO were quantified and averaged, and in animals ≥P0, the most medial 4-6 sections were quantified and averaged. Measurements and cell counts were done using ImageJ.

Counts of Tbx21+ cells in the AOB and measurements of the glomerular layer areas were performed on parasagittal sections containing identifiable glomerular layers to distinguish between anterior and posterior MCL layers. Statistical differences between genotypes were quantified with two-tailed unpaired t-test using GraphPad Prism 7.0b.

Experimental design and statistical analysis. All data were collected from mice kept under similar housing conditions, in transparent cages on a normal 12 hr light/dark cycle. Tissue collected from either males or females were analyzed and no significant sex differences were observed, so the data from males and females in the same genotype/treatment group were combined; ages analyzed are indicated in text and

figures. The data are presented as mean ± SEM. Prism 7.0b (GraphPad Software for Mac OS) was used for statistical analyses, including calculation of mean values, and standard errors. Two-tailed, unpaired t-test were used for all statistical analyses, and calculated p-values <0.05 were considered statistically significant. Sample sizes and p-values are indicated as single points in each graph and/or in figure legends.

RESULTS

AP-2ε is expressed in basal VSNs.

Immunohistochemistry on P8 mice revealed AP-2ε protein expression in the cells located in the most basal territories of the VNO (Fig 1A). Stronger AP-2ε immunoreactivity was observed in the marginal neurogenic regions of the VNO where newly formed VSNs localize proximal to the proliferating precursor cells (Fig. 1A,B, Use Fig 1K,L as reference). AP-2ε expression was also retained in mature neurons distal from the marginal zones, though at lower levels (Fig.1A,B).

The G-protein subunit Gαo is selectively expressed in differentiated basal VSNs (Herrada and Dulac, 1997; Matsunami and Buck, 1997). Double immunohistochemistry against Gαo and AP-2ε showed selective and sustained AP-2ε expression in the basal VSNs (Fig. 1C).

By using an AP-2ε$^{-/-}$ (AP-2ε–null/KO) mouse line, where the Cre recombinase transgene has been knocked in the AP-2ε coding sequence (Feng et al., 2009), we could follow the expression of non-functional AP-2ε using Cre as a proxy for AP-2ε expression. In AP-2ε$^{-/-}$ mice Cre immunoreactivity was found, as for AP-2ε in controls, strongly expressed in the marginal zones (Fig.1D,E), but in contrast to controls, cells expressing Cre were found to be distributed throughout apical and basal domains (Compare Fig.1D and A). Moreover, Cre immunoreactivity was nearly undetectable in the basal regions of the VNO distal from the marginal zones (Compare Fig.1A-D and B-E). Although Cre expression was found to overlap with AP-2ε in AP-2ε$^{+/-}$ (Fig.2A-C), no AP-2ε immunoreactivity was found in the KOs (Fig.1F).

The stronger immunoreactivity in the marginal zones suggested potential roles for AP-2ε

in differentiation or maturation steps of VSNs. To further investigate at what stages of VSN development AP-2ε is expressed (Fig. 1K-L as a reference) we performed immunolabeling against AP-2ε and the proliferative cell marker, Ki67, the neuronal precursor marker, NeuroD1, and Gap43, which labels immature neurons forming neurites (Cau et al., 2002; Cau et al., 1997; Enomoto et al., 2011; Murray et al., 2003). We detected AP-2ε protein expression restricted to post-mitotic cells at a relatively advanced stage of differentiation when Gap43 starts to be expressed and NeuroD1 is no longer immunodetectable (Fig. 1G-I,K,L).

Double immunostaining against Meis2, which is selectively expressed in apical VSNs (Chang and Parrilla, 2016; Enomoto et al., 2011), and AP-2ε revealed complementary/non-overlapping patterns of expression in apical and basal VSNs respectively (Fig. 1J-J2).

AP-2ε genetic lineage is selective for basal VSNs.

In WT animals, AP-2ε protein expression was detected only in putative basal VSNs (Fig.1 C,J). However, to understand if AP-2ε genetic lineage is exclusive for basal VSNs we took advantage of the Cre inserted in the AP-2ε locus to perform Cre-mediated genetic lineage tracing (Feng et al, 2009). Cre expression in AP-2$\varepsilon^{+/-}$ animals overlapped with AP-2ε expression both in the marginal and medial regions of the VNO (Fig2-A-C).

AP-2$\varepsilon^{+/-}$/Rosa26R lineage tracing combined with Gαo and Gαi2 immunostaining revealed that AP-2ε is expressed by cells that acquire basal identity (Fig. 2D-I). Quantifications revealed that in AP-2$\varepsilon^{+/-}$/Rosa26R, which have one AP-2ε functional allele, 98.8% SE±0.1% of the cells positive for AP-2ε lineage expressed Gαo (Fig. 2D-I).

AP-2ε loss-of-function negatively impacts the development of basal VSNs.

Whole transcript analysis on WT and AP-2$\varepsilon^{-/-}$ indicated that loss of AP-2ε leads to a downregulation of virtually all V2r genes (Fig. 3A) and to a significant increase for several V1r genes (Fig.3B). In addition, we found Gαo transcripts, which are normally expressed

by basal neurons, to be significantly decreased by 1.5-fold (p=0.01) while the apical transcription factor Meis2 appeared to be upregulated by 1.25-fold (p=0.04). Notably, Bcl11b expression remained unchanged across genotypes (data not shown). Microarray data are available in GEO (GSE110083).

These data partially overlapped with gene expression data obtained from previously described *Bcl11b* loss-of-function (Enomoto et al., 2011), which indicated further analysis of the impact of AP-2ε in controlling the basal terminal differentiation was necessary. qRT-PCR analysis confirmed a reduction in expression of basal marker Gαo ($p<0.0001$), V2R receptors, and increase in expression in the apical specific transcription factor Meis2 (p=0.01) and of V1R receptors (Fig. 3C).

We performed in-situ hybridization (ISH) against the basal marker Gαo, the apical markers Gαi2, Meis2, and against the pan VSN marker Big2 (Enomoto et al., 2011), on WT controls, and AP-2ε KOs (P21, n=3;3) (Fig. 4A-H). We also verified the protein expression of apical and basal markers Gαo, and Gαi2 via immunofluorescence (I.F) (Fig. 4O-R). In control animals, the basal marker Gαo was expressed in the basal half of the VNE (Fig.4A) whereas the apical markers Gαi2 and Meis2, were found distributed in the cells in the most apical half of the epithelium (Fig. 4C,E). However, in AP-2ε-null mice, Gαo expression was found to be reduced (Fig.4 B,P,R,T) in the basal territories of the VNE while Gαi2 and Meis2 expression covered most of the epithelium with an expression pattern comparable to the pan VSN marker, Big2 (Fig 4 B,D,F,H,I-N).

Immunofluorescent staining against Gαo and Gαi2 confirmed a dramatic reduction in cells expressing the former basal marker (Fig. 4O-R). Quantifications of the neuroepithelium after Gαo and Gαi2 double immunostaining on WT (AP-2$\varepsilon^{+/+}$), AP-2$\varepsilon^{+/-}$, and AP-2$\varepsilon^{-/-}$ (P21) indicated an overall 11% average reduction, though non-significant (p=0.2), in the total number of cells in the KO. However, a significant decrease in the number of cells expressing the basal markers together with a small increase in the number of neurons expressing apical proteins was observed in the KOs (Fig. 4 S,T). No differences in apical and basal marker expression were observed between AP-2$\varepsilon^{+/+}$ and AP-2$\varepsilon^{-/-}$ (Fig 4S).

Lack of functional AP-2ε can lead to a shift of maturing basal VSNs to the apical

differentiation program.

Performing double immunostaining against AP-2ε and the apical transcription factor Meis2 (Enomoto et al., 2011) in WT (Fig.1J-J2, Fig.5A-A2) or against Cre and Meis2 in AP-2ε$^{-/-}$ (Fig.5B-B2), we observed that in both conditions the expression of AP-2ε or Cre (in the KO) and Meis2 appeared to be mutually exclusive (Fig.5A).

This indicated that the basal program and apical differentiation program are initiated prior to, and independently from, AP-2ε expression. However, while in controls the basal neurons retained AP-2ε expression and lacked Meis2 immunoreactivity (Fig. 5A), in AP-2ε KOs Cre expression was found to be rapidly lost while Meis2 expression appears to expand to cells in the basal territories (Fig. 5B).

These data suggest that: 1) AP-2ε expression might be autoregulated and; 2) AP-2ε might have a role in silencing Meis2 expression in maturing neurons. However, in AP-2ε$^{-/-}$ mice several basal VSNs, though negative for Cre expression, were still negative for Meis2 (Fig. 5B). These data suggest that a subset of basal VSNs can acquire and maintain basal identity independently from AP-2ε expression.

AP-2εCre/R26 lineage tracing indicates that the apical transcription factor Meis2 is expressed in cells that previously entered the basal program.

AP-2εCre$^{+/-}$/R26R lineage tracing combined with Meis2 immunostaining revealed that in AP-2ε$^{+/-}$ animals occasional cells (1.4% SE±0.15, n=4) belonging to the AP-2ε lineage, were also positive for the apical marker Meis2 (Fig. 5C-C2). However, in AP-2ε$^{-/-}$ mice a significantly higher percentage (11.9%, SE±1.0, p=0.03, n=4) of all the traced cells in the VNO were positive for Meis2 expression, and notably these cells were found in both apical and basal territories of the VNO (Fig.5D-D2). This reveals that the cells that previously entered the basal program, indicated by AP-2ε lineage tracing, are capable of expressing apical markers such as Meis2, in the absence of functional AP-2ε.

The VNO undergoes massive neurogenesis in the first weeks after birth which then decreases with age (Wakabayashi and Ichikawa, 2007). Quantifications for the proliferative marker Ki67 (Fig. 5G) and for the apoptotic marker cleaved caspase-3 (P15) did not highlight differences between genotypes (Fig. 5H).

VSNs committed to the apical lineage co-express Gαo and Gαi2 while differentiating and then retain Gαi2 only as they mature (Enomoto et al., 2011). In line with this, we found putative differentiating apical VSNs in the marginal zone positive for both Gαo and Gαi2 (Fig. 5E-F2). Quantifications in controls and AP-2ε null mutants (P15) indicate a significant increase in the number of cells immunoreactive for both Gαo and Gαi2 in the AP-2$\varepsilon^{-/-}$ (Fig.5I, $p<0.0001$).

BrdU birth dating combined with genetic lineage tracing supports that lack of AP-2ε is sufficient for identity shift from basal to apical.

Immunolabeling against the V2R receptor V2R2, which is virtually expressed by all basal neurons (Martini et al., 2001), confirmed a reduction in the number of cells expressing basal cell markers in the AP-2ε null animals (Fig. 6A,B,C).

By analyzing V2R2 and Gαo expression on VNO sections of AP-2εCre$^{+/-}$/R26R and AP-2εCre$^{-/-}$/R26R traced animals we found that, while in the controls the basal markers, V2R2 and Gαo, overlap with AP-2ε lineage (Fig. 6E,H,J,L,N), in the KOs there was a significant reduction in the total number of traced cells and in the number of cells positive for AP-2ε tracing and basal markers expression (Fig. 6D,H-O). However, immunostaining against the apical marker Gαi2 and the AP-2ε tracing reporter indicated an increase in cells double positive for AP-2ε tracing and Gαi2 but negative for basal markers (Fig 6D, P-S).

To verify that the observed differences were not an artefact secondary to different penetrance of Cre recombination between AP-2$\varepsilon^{+/-}$ (one Cre allele) and AP-2$\varepsilon^{-/-}$ (two Cre alleles) we paired AP-2εCre lineage tracing, with BrdU birth dating.

BrdU injections were performed on AP-2$\varepsilon^{+/-}$/R26^{tdTomato} and AP-2$\varepsilon^{-/-}$/ R26^{tdTomato} mice at P7. Samples were collected at P21 (14 days post-injection) to age match with previous observations and cover the reported maturation rate of VSNs in mouse (de la Rosa-Prieto, 2010). Quantification of BrdU positive cells 2 weeks after injection indicate a comparable number of total BrdU+ and BrdU+/tdTomato+ positive cells between controls and KO animals (Fig. 6 E,F,G). However, while in the controls nearly all the BrdU+ cells positive for AP-2ε lineage expressed basal markers V2R2 and Gαo, in the KO only a

portion of the newly formed neurons, positive for AP-2ε lineage, were positive for the basal markers (Fig 6T). Notably, in the KO around 20% of the newly formed cells positive of the AP-2ε lineage express the apical marker Gαi2. These data corroborate that in the absence of functional AP-2ε a larger number of cells positive for AP-2ε lineage access the apical differentiation program.

AP-2ε is expressed by subsets of mitral cells of the anterior AOB. The phenotype observed in the VNO is cell autonomous

AP-2ε loss of function compromises the organization of mitral cells of the olfactory bulb (OB) (Feng et al., 2009). To understand if the observed phenotypes in the VNO could be secondary to defects in the AOB we monitored AP-2ε expression in the AOB via AP-2ε lineage tracing.

The apical VSNs express Neuropilin-2 (Nrp2) and project to the anterior AOB (a-AOB) while the basal neurons express the guidance receptor Robo2 and project to the posterior AOBs (p-AOB) (Walz et al, 2002; Prince et al, 2009). In mouse, the anterior and posterior glomerular portions of AOB are distinctly separated and are almost equal in size.

AP-2εCre linage tracing indicated that, in the AOB, the expression of the Rosa reporter was limited to the fibers of the basal VSNs projecting to the glomerular layer of the p-AOB as well as in putative mitral cells in the anterior mitral cell layer (MCL) (Fig. 7A,B,C).

Performing double immunostaining against the mitral cell marker Tbx21 (Mitsui et al., 2011; Yoshihara et al., 2005) we found that AP-2ε lineage was limited to subsets of the mitral cells only in the anterior AOB, where the apical neurons, that do not express AP-2ε, project (Fig. 7D,B,C).

By analyzing sections of traced AP-2ε$^{+/-}$ controls and AP-2ε$^{-/-}$ (KO) we observed a significant reduction in the posterior glomerular layer of the AOB (Fig. 7B,C,G) which likely reflects the reduced number of basal neurons in the VNO.

Using Tbx21 as mitral cell marker we quantified the average mitral cell numbers in controls and KO mice (Fig. 7E-F,H). These data indicated no significant effect of AP-2ε loss-of-function in the number of mitral cells.

DISCUSSION

In the last two decades, we have made significant progress in understanding cell composition, axonal guidance, and the molecular basis of chemosensory detection of the VNO (Chamero et al., 2012; Stein et al., 2016). Old or damaged VSNs are constantly replaced by newly formed cells that are incorporated into functional circuits. However, the molecular mechanisms underlying the various steps of differentiation and homeostasis of newborn neurons are not fully understood (Enomoto et al., 2011; Oboti et al., 2015).

Apical and basal VSNs originate from a common pool of progenitor cells, and transiently share common expression of the Gαo during the process of differentiation (Enomoto et al., 2011). In normal conditions, apical and basal VSNs are generated at comparable rates and numbers (Rosa-Prieto et al, 2010).

Expression of the transcription factor, AP-2ε, has been previously described in the basal cell layer of the VNO and proposed to potentially act downstream of the zinc-finger transcription protein, Bcl11b, to activate the basal VSN differentiation program and neuronal viability (Suarez, 2011). Bcl11b has been suggested to be part of a gene regulatory network responsible for initiating the basal vomeronasal program through the activation of the transcription factor AP-2ε, however this has never been further investigated.

AP-2ε is one of five members of the activating protein-2 (AP-2) family of transcription factors, which play important roles in embryonic development in a variety of tissues, including the CNS. They are often found in cell type-specific expression in either subsets of neural progenitors or postmitotic developing neurons, suggesting intrinsic roles in cell type specification, differentiation, and maintenance (Bassett et al., 2012; Feng et al., 2009; Hong et al., 2014; Kantarci et al., 2015; Pinto et al., 2009).

By analyzing a line of AP-2ε null mice we found that lack of functional AP-2ε translates into a severe reduction in expression of basal specific genes, including virtually the entire superfamily of receptors V2R and Gαo and an increase in cells expressing apical markers.

Neuronal differentiation is defined by the activation of specific transcriptional programs that are maintained throughout the life of a cell. By analyzing AP-2ε expression via immunohistochemistry and genetic lineage tracing we found that, in the VNO, AP-2ε is highly expressed in post-mitotic maturing basal neurons and that its expression is retained as the neurons mature (Fig. 1). In line with this, AP-2ε Cre lineage tracing revealed that, in AP-2$\varepsilon^{+/-}$ animals, ~99% of the cells that expressed AP-2ε acquire basal identity. Moreover, we found that AP-2ε immunodetectability does not overlap with the expression of the transcription factor Meis2, which is expressed in cells committed to become apical neurons (Enomoto et al., 2011) (Fig. 1,5) In AP-2ε null mice we found that also the non-functional AP-2ε (Cre) was expressed in maturing VSNs in the more marginal zones of the VNO with a pattern mutually exclusive with the pattern of Meis2. These data indicate that: 1) the apical-basal differentiation dichotomy starts to be established prior to AP-2ε expression and; 2) for at least some of the cells that entered the basal program, lack of Meis2 expression appears to be independent from functional AP-2ε expression (Fig. 8). However, by combining immunolabeling anti V2R2, Gαo, Meis2 with AP-2ε lineage tracing we found that, without functional AP-2ε, cells that initiated the basal VSN's program can express apical specific genes. Moreover, microarray data confirmed a decrease in expression for most the V2R genes together with an increase in transcripts for several V1R receptors.

The finding that basal VSNs can switch to the apical program was further supported in BrdU birth dating experiments combined with AP-2ε lineage tracing. In fact, 2 weeks post-BrdU injection we found that AP-2ε null mice generated a comparable number of neurons as the controls. Of the newly formed cells a similar number resulted to be positive for AP-2ε lineage tracing. However, while in controls newly formed neurons positive for AP-2ε lineage resulted to be basal neurons, only half of these were found to be positive for basal markers in the KO.

Though we could not detect significant differences in programmed cell death between genotypes we found an overall reduction of cells positive for AP-2ε tracing in the whole VNO of the KO. As both Ki67 and BrdU tracing indicate a similar neurogenic rate we

believe that the overall reduction in basal cells in the VNO of AP-2ε might be in part the result of slowly occurring increase in neuronal death (Montani et al., 2013).

The process of terminal differentiation begins as soon as the cells exit the cell cycle. During differentiation cells express identity-specific genes that progressively decrease potency and plasticity of the cells as they acquire their identity specification (Patel and Hobert, 2017). We found that AP-2ε expression turns on in post-mitotic cells after the apical-basal dichotomy has been initiated, indicated by the mutually exclusive expression of either AP-2ε or Meis2. Our lineage tracing experiments suggest that, in the vomeronasal organ, some of the cells that already enter the basal differentiation program (up to AP-2ε/Cre expression) still retain a sufficient level of cellular plasticity that allows them to abort this program, express Meis2, and switch to the alternative apical terminal differentiation program. These data suggest that AP-2ε might have the function to sustain the basal program once the apical-basal dichotomy is established.

Genetic lineage tracing using AP-2εCre$^{+/-}$ mice, which express only one functional allele of AP-2ε, revealed that even in the presence of functional AP-2ε around 1% of these cells can differentiate into apical VSNs.

This observation suggests different interpretations: 1) that a transient or under-threshold levels of AP-2ε expression might not be always sufficient to repress the apical program while undergoing basal terminal differentiation or 2) that the VSN always have a long window of plasticity and that cells that enter the basal differentiation program can default to the alternative apical program in response to genetic abnormalities, lack of connectivity, hormonal stimuli or environmental changes during the process of differentiation (Fig. 8).

Key questions that need to be answered in follow-up studies are what initiates the apical-basal dichotomy? What are the AP-2ε direct gene targets and binding partners, and what epigenetic modifications occur after AP-2ε expression during the VSNs differentiation process?

In AP-2ε null mice we observed a significant reduction but not complete loss of neurons expressing basal VSNs markers. These data indicate that, even in the absence of AP-2ε,

VSNs can initiate, the basal lineage program. These data also suggest that AP-2ε is needed to maintain basal identity for a large portion of basal VSNs but not essential for all (Fig. 8B).

Notably an incomplete ablation of basal VSNs have been also observed after loss-of-function of Ascl-1 and Ngn-1 (Cau et al., 2002), G-protein subunit Gγ-8 (Montani et al., 2013), loss-of-function of Gαo (Chamero et al., 2011), and the transcription factor ATF5 (Nakano et al., 2016). What underlies the varying responses and potential compensatory mechanisms to these mutations requires further investigation.

AP-2ε lineage tracing on AP-2ε$^{+/-}$ and AP-2ε$^{-/-}$ showed a reduced posterior AOB which, as expected, reflects the smaller number of axons projecting in the posterior AOB. However, AP-2ε is also expressed by second order olfactory neurons such as the mitral/tufted cells of the main and accessory olfactory bulb (Feng et al., 2009). AP-2ε loss-of-function affects normal olfactory bulb cell organization. The mitral/tufted cells of the aAOB and pAOB have different origins (Huilgol et al., 2013). The mitral cells of the aAOB, as those ones of the main olfactory bulb, emerge from the rostral end of the telencephalon whereas the cells of the pAOB arise from the thalamic eminence at the diencephalic-telencephalic boundary (Huilgol et al., 2013).

Our data show that, in the AOB, AP-2ε genetic lineage tracing is limited to the mitral cells of the anterior AOB, where the apical VSNs, negative for AP-2ε lineage, project. Moreover, the AP-2ε loss-of-function seem to have no effect on the total number of mitral cells in the AOB. These data support a similar lineage for the mitral cells of the aAOB to the ones of the main olfactory bulb and further suggest that the observed phenotypes in the basal VNE are cell autonomous rather than secondary to AOB defects.

In conclusion, this work demonstrated for the first time that AP-2ε is expressed in post-mitotic cells and is not required for initiating the apico-basal dichotomy but is a crucial molecular player in the progression and maintenance of the basal differentiation program. Our data suggest that AP-2ε expression in VSNs is self-maintained and needed to prevent the activation of apical specific transcription factors or their target genes. Furthermore, the early establishment the basal program suggests the existence of

unknown external regulatory inputs (e.g inductive signals, see Fig. 8) influencing terminal differentiation and cellular plasticity prior to either AP-2ε and Meis2 expression.

Further defining the inductive signals and the gene regulatory networks governing AP-2ε expression and VSN differentiation will provide important insights concerning neuronal cellular plasticity, adaptation and tuning of chemosensory epithelia to hormones (Oboti et al., 2015), experience (Xu et al., 2016) and environmental stimuli.

ACKNOWLEDGEMENTS

This work was supported by SUNY startups funds.

We thank Dr. T. Williams (Department of Craniofacial Biology, University of Colorado) for sharing the AP-2εCre mouse line. We thank Dr. J.F. Cloutier for providing plasmids to generate probes against Gαo and Gαi2. We thank Dr. R. Tirindelli (Parma University, Italy) for providing the V2R2 antibody. We also thank Dr. T. Williams, Dr. J.F. Cloutier, and Dr. R. Tirindelli additionally for their critical reading of the manuscript.

References

Bassett, E.A., Korol, A., Deschamps, P.A., Buettner, R., Wallace, V.A., Williams, T., West-Mays, J.A., 2012. Overlapping Expression Patterns and Redundant Roles for AP-2 Transcription Factors in the Developing Mammalian Retina. Developmental dynamics : an official publication of the American Association of Anatomists 241, 814-829.

Brann, J.H., Firestein, S., 2010. Regeneration of new neurons is preserved in aged vomeronasal epithelia. J Neurosci 30, 15686-15694.

Cau, E., Casarosa, S., Guillemot, F., 2002. Mash1 and Ngn1 control distinct steps of determination and differentiation in the olfactory sensory neuron lineage. Development 129, 1871-1880.

Cau, E., Gradwohl, G., Fode, C., Guillemot, F., 1997. Mash1 activates a cascade of bHLH regulators in olfactory neuron progenitors. Development 124, 1611-1621.

Chamero, P., Katsoulidou, V., Hendrix, P., Bufe, B., Roberts, R., Matsunami, H., Abramowitz, J., Birnbaumer, L., Zufall, F., Leinders-Zufall, T., 2011. G protein G(alpha)o is essential for vomeronasal function and aggressive behavior in mice. Proc Natl Acad Sci U S A 108, 12898-12903.

Chamero, P., Leinders-Zufall, T., Zufall, F., 2012. From genes to social communication: molecular sensing by the vomeronasal organ. Trends Neurosci 35, 597-606.

Chang, I., Parrilla, M., 2016. Expression patterns of homeobox genes in the mouse vomeronasal organ at postnatal stages. Gene Expr Patterns 21, 69-80.

Cloutier, J.F., Sahay, A., Chang, E.C., Tessier-Lavigne, M., Dulac, C., Kolodkin, A.L., Ginty, D.D., 2004. Differential requirements for semaphorin 3F and Slit-1 in axonal targeting, fasciculation, and segregation of olfactory sensory neuron projections. J Neurosci 24, 9087-9096.

de la Rosa-Prieto, C., Saiz-Sanchez, D., Ubeda-Banon, I., Argandona-Palacios, L., Garcia-Munozguren, S., Martinez-Marcos, A., 2010. Neurogenesis in subclasses of vomeronasal sensory neurons in adult mice. Dev Neurobiol 70, 961-970.

Enomoto, T., Ohmoto, M., Iwata, T., Uno, A., Saitou, M., Yamaguchi, T., Kominami, R., Matsumoto, I., Hirota, J., 2011. Bcl11b/Ctip2 controls the differentiation of vomeronasal sensory neurons in mice. J Neurosci 31, 10159-10173.

Feng, W., Simoes-de-Souza, F., Finger, T.E., Restrepo, D., Williams, T., 2009. Disorganized olfactory bulb lamination in mice deficient for transcription factor AP-2epsilon. Mol Cell Neurosci 42, 161-171.

Forni, P.E., Bharti, K., Flannery, E.M., Shimogori, T., Wray, S., 2013. The indirect role of fibroblast growth factor-8 in defining neurogenic niches of the olfactory/GnRH systems. J Neurosci 33, 19620-19634.

Forni, P.E., Fornaro, M., Guenette, S., Wray, S., 2011. A role for FE65 in controlling GnRH-1 neurogenesis. J Neurosci 31, 480-491.

Forni, P.E., Scuoppo, C., Imayoshi, I., Taulli, R., Dastru, W., Sala, V., Betz, U.A., Muzzi, P., Martinuzzi, D., Vercelli, A.E., Kageyama, R., Ponzetto, C., 2006. High levels of Cre expression in neuronal progenitors cause defects in brain development leading to microencephaly and hydrocephaly. J Neurosci 26, 9593-9602.

Giacobini, P., Benedetto, A., Tirindelli, R., Fasolo, A., 2000. Proliferation and migration of receptor neurons in the vomeronasal organ of the adult mouse. Brain Res Dev Brain Res 123, 33-40.
Herrada, G., Dulac, C., 1997. A novel family of putative pheromone receptors in mammals with a topographically organized and sexually dimorphic distribution. Cell 90, 763-773.
Hobert, O., 2016. Terminal Selectors of Neuronal Identity. Curr Top Dev Biol 116, 455-475.
Hong, C.S., Devotta, A., Lee, Y.H., Park, B.Y., Saint-Jeannet, J.P., 2014. Transcription factor AP2 epsilon (Tfap2e) regulates neural crest specification in Xenopus. Dev Neurobiol 74, 894-906.
Huilgol, D., Udin, S., Shimogori, T., Saha, B., Roy, A., Aizawa, S., Hevner, R.F., Meyer, G., Ohshima, T., Pleasure, S.J., Zhao, Y., Tole, S., 2013. Dual origins of the mammalian accessory olfactory bulb revealed by an evolutionarily conserved migratory stream. Nat Neurosci 16, 157-165.
Kantarci, H., Edlund, R.K., Groves, A.K., Riley, B.B., 2015. Tfap2a Promotes Specification and Maturation of Neurons in the Inner Ear through Modulation of Bmp, Fgf and Notch Signaling. PLOS Genetics 11, e1005037.
Madisen, L., Zwingman, T.A., Sunkin, S.M., Oh, S.W., Zariwala, H.A., Gu, H., Ng, L.L., Palmiter, R.D., Hawrylycz, M.J., Jones, A.R., Lein, E.S., Zeng, H., 2010. A robust and high-throughput Cre reporting and characterization system for the whole mouse brain. Nat Neurosci 13, 133-140.
Martinez-Marcos, A., Ubeda-Banon, I., Halpern, M., 2000. Cell turnover in the vomeronasal epithelium: evidence for differential migration and maturation of subclasses of vomeronasal neurons in the adult opossum. J Neurobiol 43, 50-63.
Martini, S., Silvotti, L., Shirazi, A., Ryba, N.J., Tirindelli, R., 2001. Co-expression of putative pheromone receptors in the sensory neurons of the vomeronasal organ. J Neurosci 21, 843-848.
Matsunami, H., Buck, L.B., 1997. A multigene family encoding a diverse array of putative pheromone receptors in mammals. Cell 90, 775-784.
Mitsui, S., Igarashi, K.M., Mori, K., Yoshihara, Y., 2011. Genetic visualization of the secondary olfactory pathway in Tbx21 transgenic mice. Neural Syst Circuits 1, 5.
Montani, G., Tonelli, S., Sanghez, V., Ferrari, P.F., Palanza, P., Zimmer, A., Tirindelli, R., 2013. Aggressive behaviour and physiological responses to pheromones are strongly impaired in mice deficient for the olfactory G-protein -subunit G8. J Physiol 591, 3949-3962.
Murray, R.C., Navi, D., Fesenko, J., Lander, A.D., Calof, A.L., 2003. Widespread defects in the primary olfactory pathway caused by loss of Mash1 function. J Neurosci 23, 1769-1780.
Nakano, H., Iida, Y., Suzuki, M., Aoki, M., Umemura, M., Takahashi, S., Takahashi, Y., 2016. Activating transcription factor 5 (ATF5) is essential for the maturation and survival of mouse basal vomeronasal sensory neurons. Cell Tissue Res 363, 621-633.
Oboti, L., Ibarra-Soria, X., Perez-Gomez, A., Schmid, A., Pyrski, M., Paschek, N., Kircher, S., Logan, D.W., Leinders-Zufall, T., Zufall, F., Chamero, P., 2015. Pregnancy and estrogen enhance neural progenitor-cell proliferation in the vomeronasal sensory epithelium. BMC Biol 13, 104.
Patel, T., Hobert, O., 2017. Coordinated control of terminal differentiation and restriction of cellular plasticity. Elife 6.
Pinto, L., Drechsel, D., Schmid, M.T., Ninkovic, J., Irmler, M., Brill, M.S., Restani, L., Gianfranceschi, L., Cerri, C., Weber, S.N., Tarabykin, V., Baer, K., Guillemot, F., Beckers, J., Zecevic, N., Dehay, C., Caleo, M., Schorle, H., Gotz, M., 2009. AP2gamma regulates basal

progenitor fate in a region- and layer-specific manner in the developing cortex. Nat Neurosci 12, 1229-1237.
Silvotti, L., Moiani, A., Gatti, R., Tirindelli, R., 2007. Combinatorial co-expression of pheromone receptors, V2Rs. J Neurochem 103, 1753-1763.
Srinivas, S., Watanabe, T., Lin, C.S., William, C.M., Tanabe, Y., Jessell, T.M., Costantini, F., 2001. Cre reporter strains produced by targeted insertion of EYFP and ECFP into the ROSA26 locus. BMC Dev Biol 1, 4.
Stein, B., Alonso, M.T., Zufall, F., Leinders-Zufall, T., Chamero, P., 2016. Functional Overexpression of Vomeronasal Receptors Using a Herpes Simplex Virus Type 1 (HSV-1)-Derived Amplicon. PLoS One 11, e0156092.
Suarez, R., 2011. Molecular switches in the development and fate specification of vomeronasal neurons. J Neurosci 31, 17761-17763.
Tirindelli, R., Ryba, N.J., 1996. The G-protein gamma-subunit G gamma 8 is expressed in the developing axons of olfactory and vomeronasal neurons. Eur J Neurosci 8, 2388-2398.
Wakabayashi, Y., Ichikawa, M., 2007. Distribution of Notch1-expressing cells and proliferating cells in mouse vomeronasal organ. Neurosci Lett 411, 217-221.
Xu, P.S., Lee, D., Holy, T.E., 2016. Experience-Dependent Plasticity Drives Individual Differences in Pheromone-Sensing Neurons. Neuron 91, 878-892.
Yoshihara, S., Omichi, K., Yanazawa, M., Kitamura, K., Yoshihara, Y., 2005. Arx homeobox gene is essential for development of mouse olfactory system. Development 132, 751-762.

Figure 1: AP-2ε is expressed in differentiating basal vomeronasal sensory neurons (VSNs)

Immunohistochemistry against AP-2ε, P8 WT, (A) AP-2ε was expressed in the marginal and intermediate regions of the VNO (segments 1,2,6,7) and at lower levels in the more medial basal regions of the VNO (segments 3,4,5) (B) Quantification of optic density (OD) indicating differential AP-2ε immunoreactivity in the different regions of the VNO, zone numbers refer to the zones as indicated in A, each point represents average OD quantifications from independent VNE (A), values normalized to the OD of zone 1. C) Double immunofluorescence against AP-2ε and Gαo on P21 WT shows AP-2ε expression (red) in Gαo positive basal neurons (green, arrowhead). D) Immunohistochemistry against Cre on AP-2εCre KO (P8) shows strong expression of Cre at the marginal and intermediate zones (segments 1,2,6,7) but nearly complete absence of Cre immunodetectability in the medial/central regions of the VNO (zones 3,4,5). E) Quantification of OD indicating different Cre immunoreactivity in the different zones as in (D). (H-J2) Double immunofluorescence on WT against AP-2ε and Ki67 (H-H2), shows lack of AP-2ε expression (red, arrowheads) in proliferating cells (green, arrows). (I-I2) Immunofluorescence against AP-2ε (red, arrowheads) and NeuroD1 (green, arrows) shows lack of colocalization. (I-I2) Immunofluorescence against AP-2ε (red) and Gap43 (green) shows that AP-2ε is expressed in Gap43+ cells (arrows). J-J2) Double immunofluorescence on WT against AP-2ε (red) and Meis2 (green) shows lack of colocalization in the neurogenic niche and a topographic distinction as the VSNs mature and migrate into the medial portions of the VNO (arrows). K) Schematic of the VNO. Zones 1,7 indicate the marginal zones where neurogenesis and differentiation of neurons occur. L) Cartoon summarizing key differentiation steps of VSNs Ascl1+ neural progenitor cells (purple) reside in the progress through maturation stages. AP-2ε immunoreactivity starts after NeuroD1 as Gap43 starts to be expressed. Mature Meis2+ apical (green) and AP-2ε+ basal neurons (red) migrate towards the central zones with increasing expression of olfactory marker protein as they mature (Zone 3-5).

Figure 2: AP-2ε lineage is selective for basal vomeronasal sensory neurons in the vomeronasal organ

A-C) AP-2ε/Cre double immunostaining on P15 AP-2ε$^{+/-}$, AP-2ε (green, B) and Cre (magenta, C) show overlapping AP-2ε and Cre expression in the basal regions of the VNO (arrow). Sparse cells positive for both AP-2ε and Cre were found in the apical region (arrowhead). D-F) Double immunostaining on P15 postnatal AP-2εCre$^{+/-}$/R26YFP VNOs against YFP (red) and Gαi2(green). YFP (red) shows AP-2εCre lineage in the basal (b) territories of the VNO (a) but not in the apical (a) cells expressing Gαi2 (green). Arrowhead points to a single neuron positive for AP-2ε in apical region. (G-I) Double immunostaining against YFP (red) and Gαo (green) shows co-localization between AP-2εCre lineage reporter and the basal (b) cell marker Gαo. Arrowhead indicates a single neuron positive for AP-2ε tracing negative for basal marker.

Figure 3: Microarray data and qRT-PCR data

Affymetrix Mouse Gene ST 2.0 microarray data (WT n=3; KO n=3). Volcano plot of V2r (A) and V1r (B) vomeronasal receptor genes expression. Individual vomeronasal receptor genes are plotted against the negative $\log_{10}$ of the adjusted P-value ($-\log_{10}(p=0.05)=1.30$; dashed line) against the fold change. All the genes other than V1r and V2rs are represented in gray. All values with a fold change <-1.1 are indicated in green and considered to be significantly down-regulated if $p<0.05$ while genes with a fold change >1.1 (red) and considered to be significantly up-regulated. Of the 134 V2r receptors genes expressed, 75% were found to be significantly down-regulated. Of the 213 V1r receptor genes expressed, 5% were found to be significantly upregulated. C) qRT-PCR indicates a decrease in expression for basal markers Gαo ($p<0.0001$), Vmn2r receptors in AP-2ε null mice together with a significant increase of expression for the apical transcription factor Meis2 and Vmn1rs receptors. Gene expression was normalized to Gapdh before statistical analysis by two-tailed, unpaired t-test

Figure 4: AP-2ε loss-of-function disrupts basal vomeronasal sensory neuron development

A-B) In situ hybridization against Gαo on A) WT shows robust Gαo expression (red dotted line) in the basal portion of the VNE. B) AP-2ε KO displays a marked reduction of neuroepithelium positive for Gαo mRNA expression in comparison to WT (black arrow), I,J) High magnification images of Gαo ISH on I) WT and J) AP-2ε KO. C-D) ISH against Gαi2 on C) WT VNO shows the Gαi2 expression (red dotted line) in the apical portion of the neuroepithelium. In the AP-2ε KO, an apparent expansion of the Gαi2 expressing area (black arrow) was observed when compared to WT. O,P) High magnification images of Gαi2 ISH on O) WT and P) KO. E-H) Double immunofluorescence against Gαo (red) and Gαi2 (green) on WT (E,G) display a comparable number of basal and apical VSNs in the neuroepithelium. In the AP-2ε KO (F,H) a significant reduction of the Gαo+ basal population (white arrows) and apparent expansion of the Gαi2+ apical population. ISH against I-J) Meis2 shows a similar expression to Gαi2 in the apical portion of the I) WT vomeronasal epithelium. J) In the AP-2ε KO we observe a similar expansion of Meis2 expression, Q, R) high magnification images of Q) WT and R) AP-2ε KO. ISH against K,L) Big2, which is expressed throughout the vomeronasal epithelium, shows comparable maintained expression between K) WT and L) AP-2ε KO mice. S) Quantifications of average number of Gαo+, Gαi2+, and total number of VSNs in the neuroepithelium of P21 WT and AP-2ε KO mice. In the AP-2ε KO, a significant decrease in the number of Gαo+ basal neurons ($p=0.009$) and increase in the number of Gαi2+ apical neurons ($p=0.0008$), with no change in total number of VSNs per section ($p=0.2$). T) Quantifications of apical, basal, and total neuroepithelium thickness (μm) in P21 WT and AP-2ε KO VNE similarly show significant decrease in the average

neuroepithelium thickness of the basal VSN population ($p<0.0001$) and an increase in the apical population of VSNs ($p=0.006$), with no significant difference in total epithelium thicknesses. Statistical analysis by two-tailed, unpaired t-test.

Figure 5: An increase in Gαo/Gαi2 double positive cells indicate increase in apical neuronal precursors.

Double immunofluorescence against A) AP-2ε (red) and Meis2 (green) on P21 WT shows that AP-2ε and Meis2 do not colocalize in newly generated post-mitotic cells (notched arrows) and remain mutually exclusive in mature neurons located medially in the VNE (white arrows). B) Double immunofluorescence against Cre (red) and Meis2 (green) on P21 AP-2ε$^{-/-}$ show a similar pattern (notched arrows). However, while AP-2ε expression persists in mature basal VSNs, Cre immunodetectability fades in more medial regions (white arrows) while the region of Meis2+ cells appears to increase. C,D) Double immunofluorescence against AP-2ε lineage tracing (red) and Meis2 (green) on C) AP-2ε$^{+/-}$/R26R^{YFP} shows few cells positive for AP-2ε lineage that also express Meis2. D) AP-2ε$^{-/-}$/R26R^{YFP} shows a higher frequency of AP-2ε lineage traced cells that also express Meis2 in both apical and basal regions when compared to controls (arrowheads).

E-F2) Double immunofluorescence against Gαo and Gαi2 on P21 AP-2ε E) WT VNOs show the immature VSNs that are positive for both Gαo and Gαi2, however in F) AP-2ε null animals, the average number of these double positive cells significantly increases when compared to both WT and AP-2ε$^{-/-}$ controls (I, $p<0.0001$). G) Quantifications on P15 AP-2ε WT and KO VNOs for G) average number of proliferating cells (Ki67+) per section reveals no significant changes in the number of newly generated neurons ($p=0.8$). H) Quantifications on P15 AP-2ε WT and KO VNOs for the average number of apoptotic (Cleaved-Caspase-3+) cells showed no significant difference in the number of cells undergoing programmed cell death ($p=0.3$). Statistical analysis by two-tailed, unpaired t-test.

Figure 6: AP-2εCre null mice show a higher number of cells positive AP-2ε lineage that acquire apical-like characteristics

A,B) Immunofluorescence against V2R2 (red) on P21 AP-2ε WT (A) and AP-2ε $^{-/-}$ (B) shows a dramatic reduction in the cells positive for V2R2. C) Quantification of number of V2R2+ and OMP cells/section shows a significant reduction in V2R2+ cells in AP-2ε $^{-/-}$ ($p=0.004$) but non-significant reduction in the total number of mature VSNs positive for OMP.

D) Quantification of total AP-2εCre traced cells, traced cells positive for V2R2 expression and Gαi2 expression in AP-2ε$^{+/-}$/R26^{tdTomato} controls and AP-2ε$^{-/-}$/R26^{tdTomato} (Null). Data show a significant reduction in cells positive for AP-2ε tracing in the KO as well as in the number of cells expressing the basal marker V2R2. In the KO there is a similar significant increase in traced cells negative for V2R2 and in cells expressing the apical marker Gαi2. E-F) Representative image of immunostainings against AP-2ε lineage tracing (tdTomato, red), V2R2 (green), and BrdU (white) at P21 on AP-2ε$^{+/-}$

/R26^{tdTomato} (D) and AP-2ε$^{-/-}$/R26^{tdTomato}. G) Quantification of neurons formed 2 weeks after BrdU injection. The number of newly born neurons and the number of BrdU+ AP-2ε lineage traced neurons are similar between AP-2ε$^{+/-}$/R26^{tdTomato} controls and AP-2ε$^{-/-}$ R26^{tdTomato}.
H-K) Double immunofluorescence against the Rosa reporter tdTomato (magenta) and V2R2 (green) on P21 AP-2ε$^{+/-}$/R26^{tdTomato} (H,J) show colocalization in the basal region of the epithelium (arrow). Sparse cells positive for AP-2ε lineage negative for V2R2 (arrowheads) were detected in apical region. (I,K) A large number of AP-2ε traced cells (magenta) are negative for V2R2 expression in both basal and apical territories (arrowheads).
L-O) Double immunofluorescence against the Rosa reporter tdTomato (magenta) and Gαo (green). L,N) P21 AP-2ε$^{+/-}$/R26^{tdTomato} show tdTomato and Gαo colocalization in the basal region of the epithelium (arrow). (M,O) In AP-2ε null mice a large number of AP-2ε traced cells (magenta) are negative for Gαo expression in both basal and apical territories (arrowheads).
P-S) AP-2ε lineage tracing (magenta) and Gαi2 expression (green) in P21 AP-2ε$^{+/-}$ /R26^{tdTomato} (P,R) show cells positive for AP-2ε lineage in the basal half of the VNE do not express the apical marker Gαi2 (arrow). (Q,S) AP-2ε$^{-/-}$/R26^{tdTomato} VNE several cells positive for AP-2ε lineage (magenta) are positive for Gαi2 (arrowheads).
T) Quantification of BrdU labelled cells 2 weeks after BrdU injection positive AP-2ε lineage, basal markers (V2R and Gαo) and apical marker (Gαi2). Data show a reduction in basal marker expression in the KO (V2R2+ p-0.0005; Gαo, p<0.0001) and a small but a significant increase in the number of BrdU+/lineage traced cells that express the apical marker (Gαi2, p=0.03). Statistical analysis by two-tailed, unpaired t-test.

Figure 7: The glomerular layer of the posterior accessory olfactory bulb is reduced with no significant changes to the anterior glomerular layer or mitral/tufted cell layers

A) Immunohistochemistry against YFP (brown)on parasagittal sections of the AOB of AP-2ε$^{+/-}$/R26YFP (P21) shows the basal vomeronasal fibers projecting to the posterior glomerular layer (GL) of the AOB along with cell bodies in the anterior mitral cell layer (MCL) (black arrow heads) (black notched arrow) but into the posterior MCL (regions traced with black dotted line).
B,C) Immunofluorescence against Nrp2 (green) and lineage tracing (magenta) on B) AP-2ε$^{+/-}$/R26YFP and C) AP-2ε$^{-/-}$/R26YFP mice. Axons from the apical neurons (Nrp2+) populate the anterior GL of the AOB in both AP-2ε$^{+/-}$ and AP-2ε null animals. Traced fibers from the VNO defasciculate at the border between the anterior AOB (a-AOB) and posterior AOB (p-AOB) (notched arrow). C) Reduced posterior (p) GL was observed in AP-2ε null mice compared to controls (B), see quantification in (G). D) Immunostaining against the mitral cell marker, Tbx21 (green), and the R26 marker YFP (magenta). Tbx21+ mitral cells negative for the AP-2ε lineage (notched arrow) were found throughout the anterior and posterior MCL, however a subpopulation of mitral cells was observed to be positive for the AP-2ε lineage tracing (white arrows), but was restricted

to the anterior portion of the MCL, (a-MCL and p-MCL marked separated by white dotted line).
E,F) Immunostaining against the mitral cell marker, Tbx21 (green) and YFP (magenta) on AOBs of AP-2$\varepsilon^{+/-}$/R26YFP (E) and AP-2$\varepsilon^{-/-}$/R26YFP (F) show Tbx21+ mitral cells throughout the anterior and posterior MCL in both genotypes (quantification in H).
G) Quantification of the average area of GL of the AOB in AP-2$\varepsilon^{+/-}$/R26YFP and AP-2$\varepsilon^{-/-}$/R26YFP shows non-significant difference in the a-AOB between genotypes ($p=0.1$), but significant reduction in p-AOB of AP-2εKO ($p<0.0001$). H) Quantifications of the total number of Tbx21+ cells in the MCL of AP-2$\varepsilon^{+/-}$/R26YFP and AP-2$\varepsilon^{-/-}$/R26YFP showed non-significant decrease in the posterior MCL ($p=0.09$). Statistical analysis by two-tailed, unpaired t-test.

Figure 8: Cartoons illustrating a model of terminal differentiation. A) Early postmitotic neurons are directed, potentially by local inductive signals, to initiate either the apical or basal differentiation program and express either AP-2ε (basal transcription factor) or Meis2 (apical transcription factor). AP-2ε alone or together other unknown factors (?) blocks the expression of apical genes, e.g. Meis2. AP-2ε expression is self-sustained (see Fig.1). Meis2 expression might play a similar/opposite role to the one of AP-2ε by repressing AP-2ε expression once established in differentiating apical neurons.
B) In the absence of AP-2ε the apical-basal dichotomy is established in the KOs as Cre (nonfunctional AP-2ε) and Meis2 are expressed in a mutually exclusive fashion (See Figure 5).
In the absence of functional AP-2ε some differentiating basal VSNs remain negative for Meis2 suggesting that other unknown factors (?) may compensate the lack of AP-2ε and maintain the basal identity. In some basal VSNs (green and purple) Meis2 is expressed and activates apical genes.

Table 1: qRT-PCR Primer Sequences
Sequences of primers used in qRT-PCR analysis (see Fig. 3C) for Gαo, Meis2, Vmn1r81, Vmn1r84, Vmn2r69, Vmn2r18, and Gapdh.

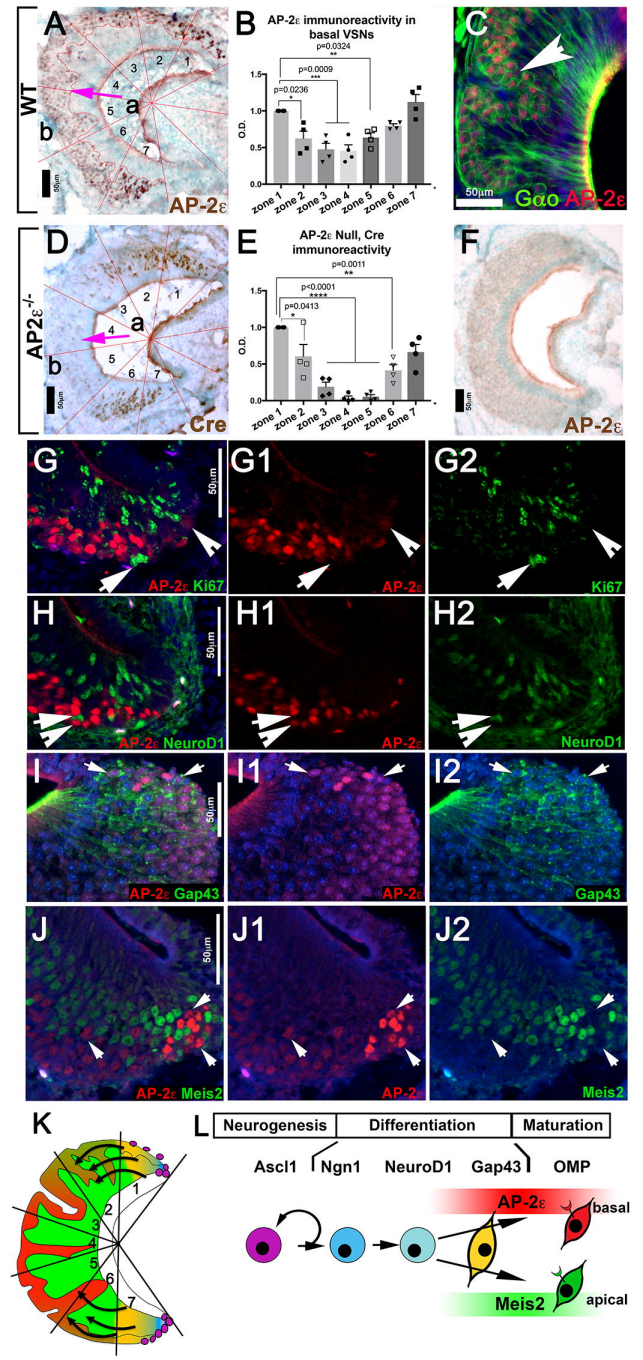
A
WT
a
b
1
2
3
4
5
6
7
50µm
AP-2ε
B
AP-2ε immunoreactivity in basal VSNs
p=0.0324
**
p=0.0009
***
p=0.0236
*
O.D.
1.5
1.0
0.5
0.0
zone 1
zone 2
zone 3
zone 4
zone 5
zone 6
zone 7
C
50µm
Gαo AP-2ε
D
AP2ε-/-
a
b
1
2
3
4
5
6
7
50µm
Cre
E
AP-2ε Null, Cre immunoreactivity
p=0.0011
**
p<0.0001
****
p=0.0413
*
O.D.
1.5
1.0
0.5
0.0
zone 1
zone 2
zone 3
zone 4
zone 5
zone 6
zone 7
F
50µm
AP-2ε
G
50µm
AP-2ε Ki67
G1
AP-2ε
G2
Ki67
H
50µm
AP-2ε NeuroD1
H1
AP-2ε
H2
NeuroD1
I
50µm
AP-2ε Gap43
I1
AP-2ε
I2
Gap43
J
50µm
AP-2ε Meis2
J1
AP-2ε
J2
Meis2
K
1
2
3
4
5
6
7
L
Neurogenesis
Differentiation
Maturation
Ascl1
Ngn1
NeuroD1
Gap43
OMP
AP-2ε
basal
Meis2
apical

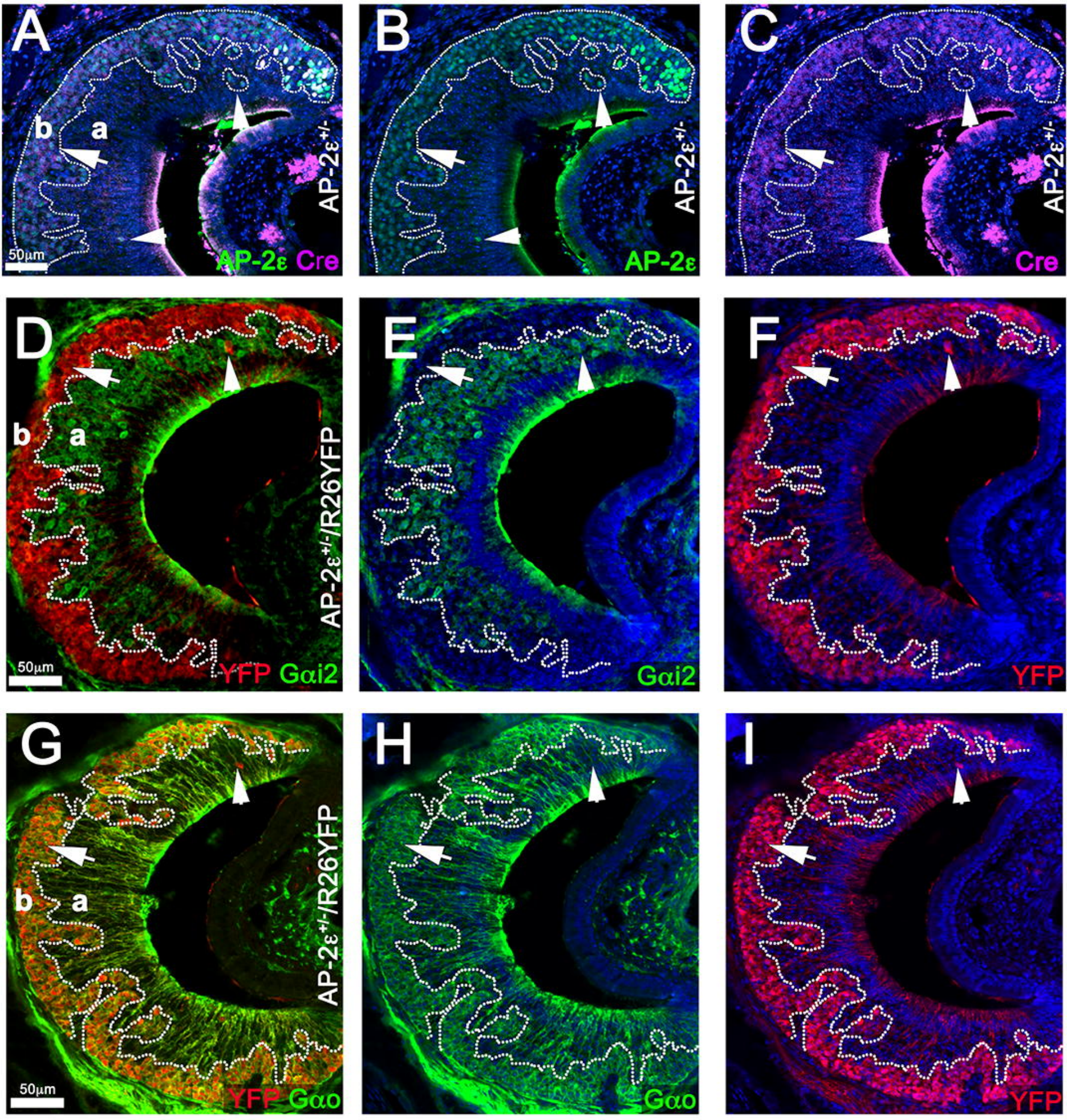
A
b
a
AP-2ε+/-
50μm
AP-2ε Cre
B
AP-2ε+/-
AP-2ε
C
AP-2ε+/-
Cre
D
b
a
AP-2ε+/-/R26YFP
50μm
YFP Gαi2
E
Gαi2
F
YFP
G
b
a
AP-2ε+/-/R26YFP
50μm
YFP Gαo
H
Gαo
I
YFP

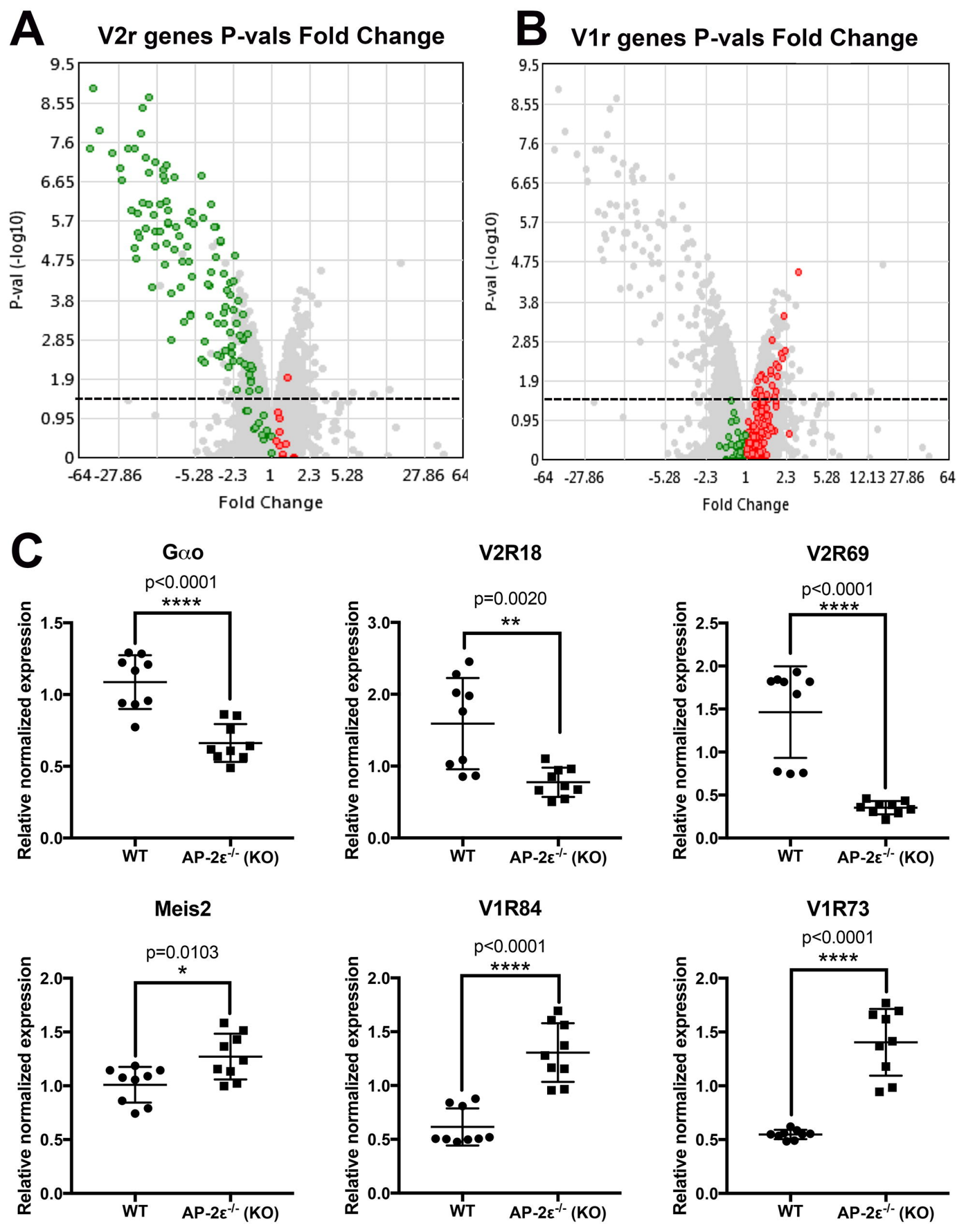
A
V2r genes P-vals Fold Change
P-val (-log10)
9.5
8.55
7.6
6.65
5.7
4.75
3.8
2.85
1.9
0.95
0
-64 -27.86 -5.28 -2.3 1 2.3 5.28 27.86 64
Fold Change
B
V1r genes P-vals Fold Change
P-val (-log10)
9.5
8.55
7.6
6.65
5.7
4.75
3.8
2.85
1.9
0.95
0
-64 -27.86 -5.28 -2.3 1 2.3 5.28 12.13 27.86 64
Fold Change
C
Gαo
p<0.0001
****
Relative normalized expression
1.5
1.0
0.5
0.0
WT
AP-2ε-/- (KO)
V2R18
p=0.0020
**
Relative normalized expression
3.0
2.0
1.0
0.0
WT
AP-2ε-/- (KO)
V2R69
p<0.0001
****
Relative normalized expression
2.5
2.0
1.5
1.0
0.5
0.0
WT
AP-2ε-/- (KO)
Meis2
p=0.0103
*
Relative normalized expression
2.0
1.5
1.0
0.5
0.0
WT
AP-2ε-/- (KO)
V1R84
p<0.0001
****
Relative normalized expression
2.0
1.5
1.0
0.5
0.0
WT
AP-2ε-/- (KO)
V1R73
p<0.0001
****
Relative normalized expression
2.0
1.5
1.0
0.5
0.0
WT
AP-2ε-/- (KO)

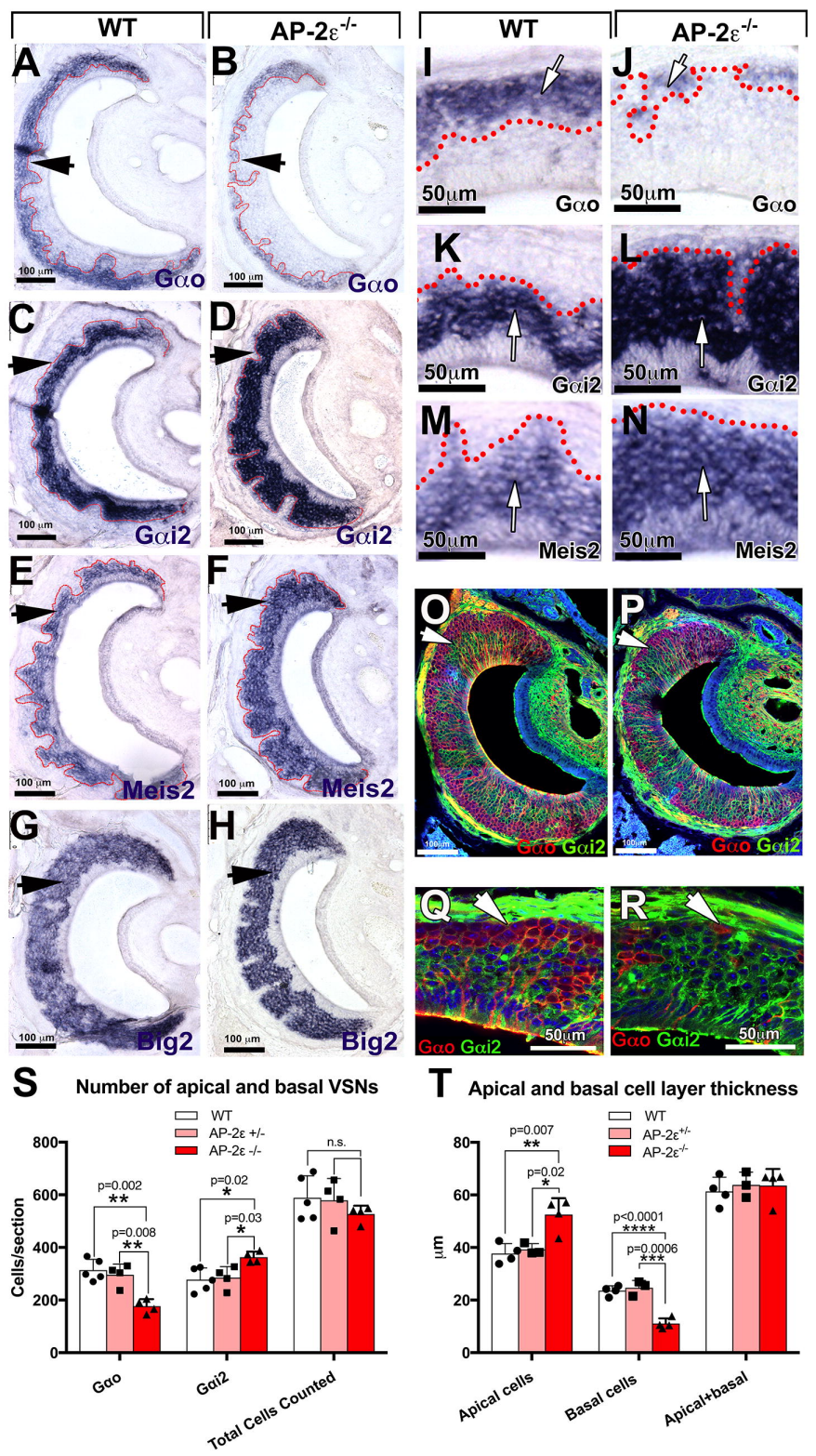
WT
AP-2ε-/-
A
B
Gαo
C
D
Gαi2
E
F
Meis2
G
H
Big2
100 μm
I
J
K
L
M
N
50μm
O
P
Gαo Gαi2
Q
R
S
Number of apical and basal VSNs
WT
AP-2ε +/-
AP-2ε -/-
Cells/section
p=0.002
p=0.008
p=0.02
p=0.03
n.s.
Gαo
Gαi2
Total Cells Counted
T
Apical and basal cell layer thickness
AP-2ε+/-
AP-2ε-/-
μm
p=0.007
p=0.02
p<0.0001
p=0.0006
Apical cells
Basal cells
Apical+basal

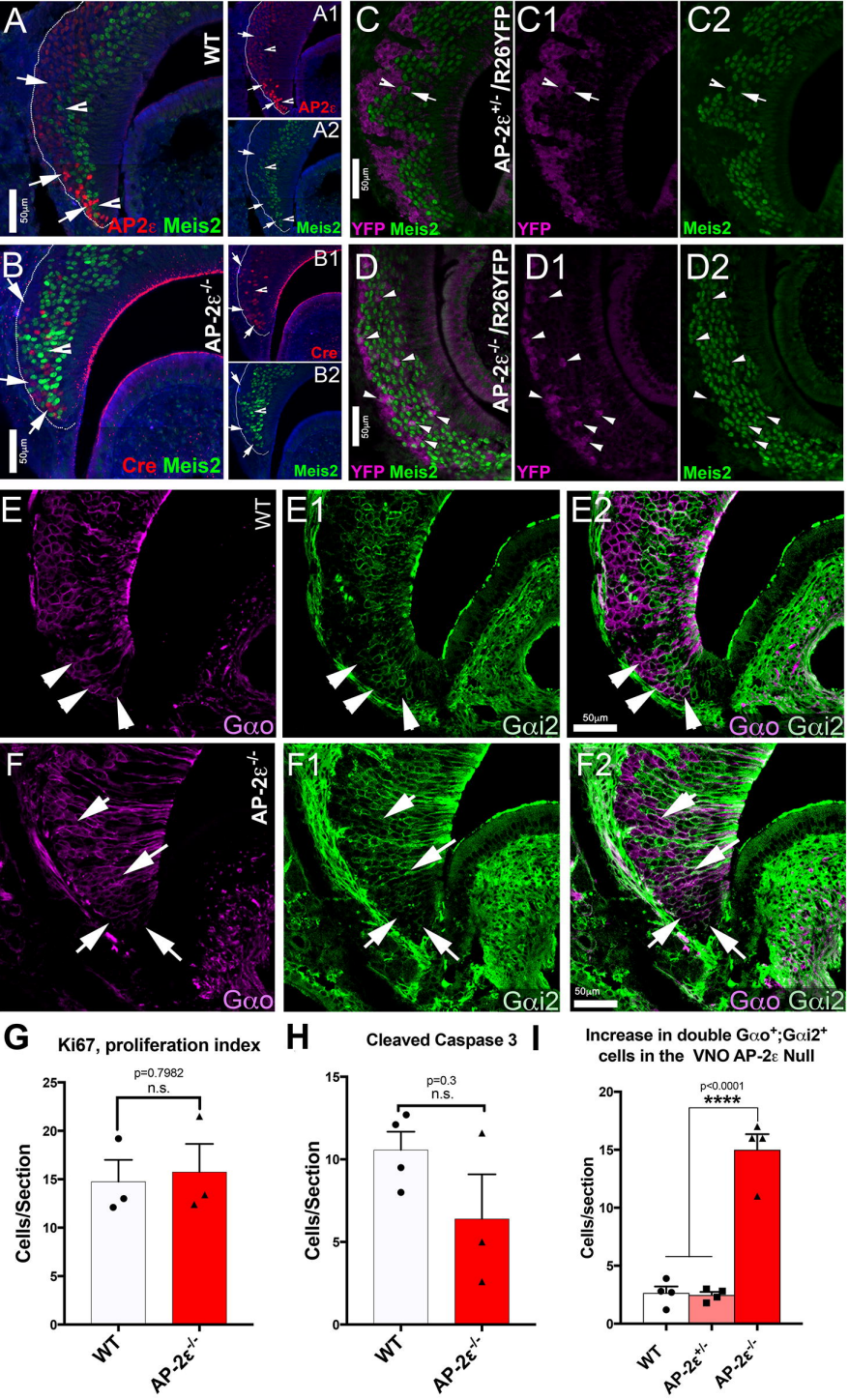
A
WT
A1
AP2ε
A2
Meis2
AP2ε Meis2
50μm
C
AP-2ε+/- /R26YFP
C1
C2
YFP Meis2
YFP
Meis2
B
AP-2ε-/-
B1
Cre
B2
Meis2
Cre Meis2
D
AP-2ε-/- /R26YFP
D1
D2
YFP Meis2
YFP
Meis2
E
WT
E1
E2
Gαo
Gαi2
Gαo Gαi2
F
AP-2ε-/-
F1
F2
Gαo
Gαi2
Gαo Gαi2
G
Ki67, proliferation index
p=0.7982
n.s.
Cells/Section
WT
AP-2ε-/-
H
Cleaved Caspase 3
p=0.3
n.s.
Cells/Section
WT
AP-2ε-/-
I
Increase in double Gαo+;Gαi2+ cells in the VNO AP-2ε Null
p<0.0001
****
Cells/section
WT
AP-2ε+/-
AP-2ε-/-

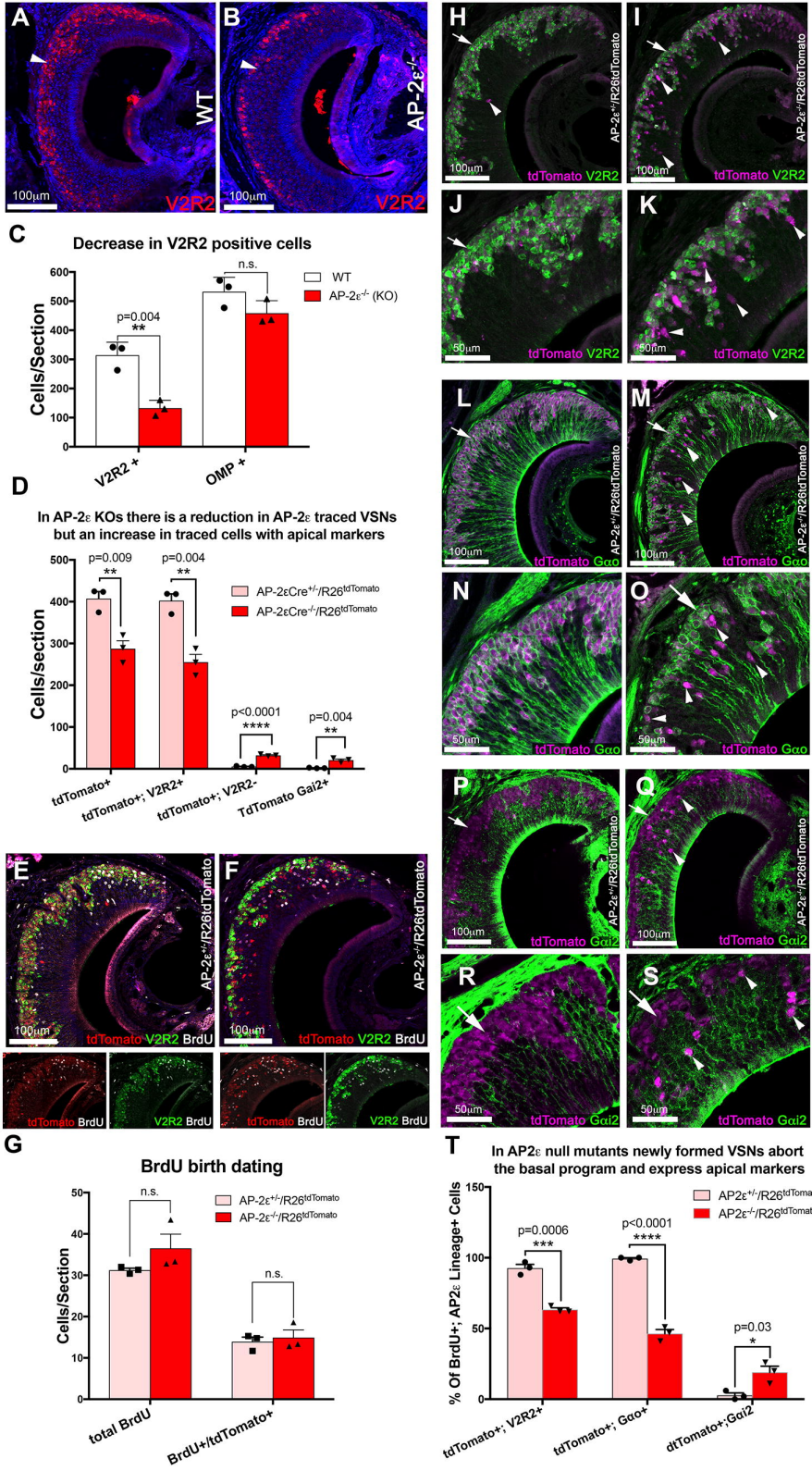
A
WT
100μm
V2R2
B
AP-2ε-/-
100μm
V2R2
C
Decrease in V2R2 positive cells
Cells/Section
600
500
400
300
200
100
0
p=0.004
**
n.s.
WT
AP-2ε-/- (KO)
V2R2 +
OMP +
D
In AP-2ε KOs there is a reduction in AP-2ε traced VSNs
but an increase in traced cells with apical markers
Cells/section
500
400
300
200
100
0
p=0.009
**
p=0.004
**
AP-2εCre+/-/R26tdTomato
AP-2εCre-/-/R26tdTomato
p<0.0001
****
p=0.004
**
tdTomato+
tdTomato+; V2R2+
tdTomato+; V2R2-
TdTomato Gαi2+
E
AP-2ε+/-/R26tdTomato
100μm
tdTomato V2R2 BrdU
tdTomato BrdU
V2R2 BrdU
F
AP-2ε-/-/R26tdTomato
100μm
tdTomato V2R2 BrdU
tdTomato BrdU
V2R2 BrdU
G
BrdU birth dating
Cells/Section
50
40
30
20
10
0
n.s.
n.s.
AP-2ε+/-/R26tdTomato
AP-2ε-/-/R26tdTomato
total BrdU
BrdU+/tdTomato+
H
AP-2ε+/-/R26tdTomato
100μm
tdTomato V2R2
I
AP-2ε-/-/R26tdTomato
100μm
tdTomato V2R2
J
50μm
tdTomato V2R2
K
50μm
tdTomato V2R2
L
AP-2ε+/-/R26tdTomato
100μm
tdTomato Gαo
M
AP-2ε-/-/R26tdTomato
100μm
tdTomato Gαo
N
50μm
tdTomato Gαo
O
50μm
tdTomato Gαo
P
AP-2ε+/-/R26tdTomato
100μm
tdTomato Gαi2
Q
AP-2ε-/-/R26tdTomato
100μm
tdTomato Gαi2
R
50μm
tdTomato Gαi2
S
50μm
tdTomato Gαi2
T
In AP2ε null mutants newly formed VSNs abort
the basal program and express apical markers
% Of BrdU+; AP2ε Lineage+ Cells
150
100
50
0
p=0.0006
***
p<0.0001
****
p=0.03
*
AP2ε+/-/R26tdTomato
AP2ε-/-/R26tdTomato
tdTomato+; V2R2+
tdTomato+; Gαo+
dtTomato+;Gαi2

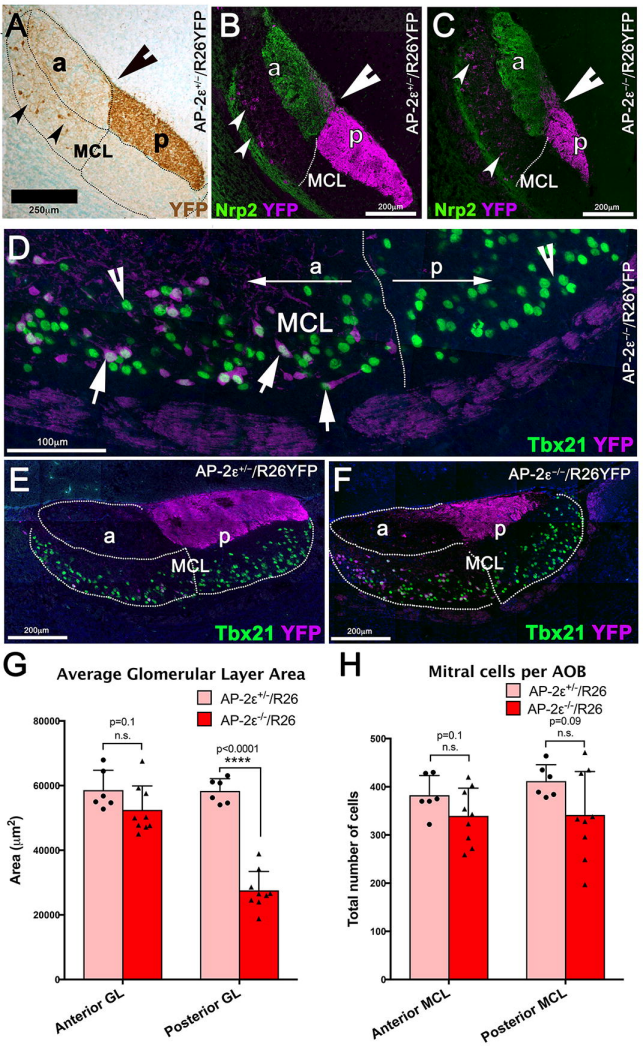
A
a
MCL
p
250µm
YFP
B
AP-2ε+/-/R26YFP
a
p
MCL
200µm
Nrp2 YFP
C
AP-2ε-/-/R26YFP
a
p
MCL
200µm
Nrp2 YFP
D
a
p
MCL
AP-2ε-/-/R26YFP
100µm
Tbx21 YFP
E
AP-2ε+/-/R26YFP
a
p
MCL
200µm
Tbx21 YFP
F
AP-2ε-/-/R26YFP
a
p
MCL
200µm
Tbx21 YFP
G
Average Glomerular Layer Area
AP-2ε+/-/R26
AP-2ε-/-/R26
p=0.1
n.s.
p<0.0001
****
Area (µm²)
80000
60000
40000
20000
0
Anterior GL
Posterior GL
H
Mitral cells per AOB
AP-2ε+/-/R26
AP-2ε-/-/R26
p=0.1
n.s.
p=0.09
n.s.
Total number of cells
500
400
300
200
100
0
Anterior MCL
Posterior MCL

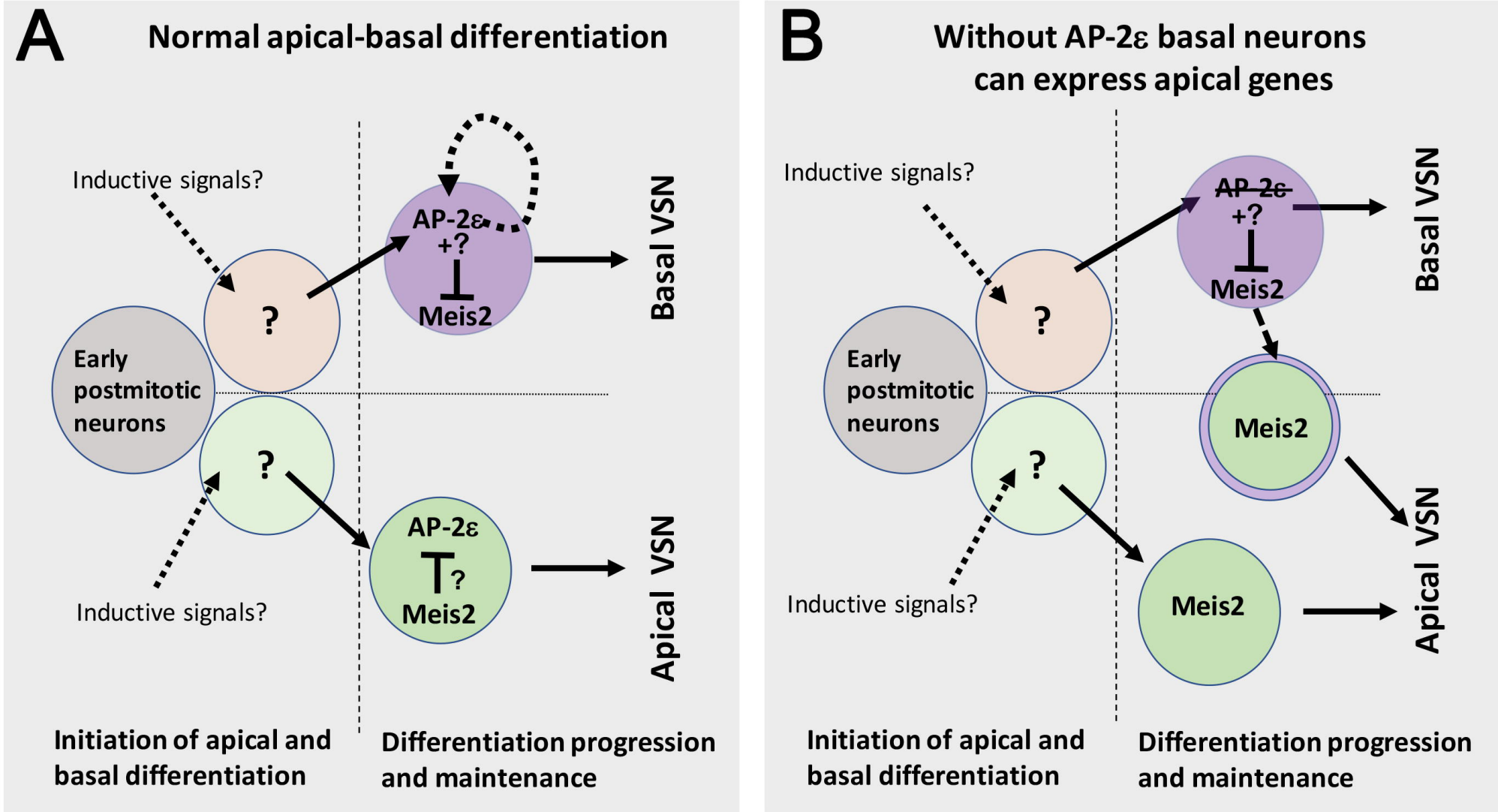
A
Normal apical-basal differentiation
Inductive signals?
?
AP-2ε
+?
Meis2
Basal VSN
Early
postmitotic
neurons
?
AP-2ε
T?
Meis2
Inductive signals?
Apical VSN
Initiation of apical and
basal differentiation
Differentiation progression
and maintenance
B
Without AP-2ε basal neurons
can express apical genes
Inductive signals?
?
AP-2ε
+?
Meis2
Basal VSN
Early
postmitotic
neurons
?
Meis2
Inductive signals?
Meis2
Apical VSN
Initiation of apical and
basal differentiation
Differentiation progression
and maintenance

Table 1: qRT-PCR Primer Sequences

SEQUENCE (5' ➔ 3')	GENE
CAGCCTGGATCGGATTGG	Guanine nucleotide binding protein, alpha O (Gαo) FWD
TGACTCTGGTTCGGAGGATGT	Guanine nucleotide binding protein, alpha O (Gαo) REV
TGAGCAAGGCGATGGGTTAG	Meis homeobox 2 FWD
TGTCTGGATCGTCGTCATCAC	Meis homeobox 2 REV
TGCCTACTGGGTTGTTTCCAA	Vomeronasal 1 receptor 81 FWD
TTGTGGCTCTGTGTTTAAGCATAAT	Vomeronasal 1 receptor 81 REV
CTCCTGGATGACCTCTTATGTAAACTT	Vomeronasal 1 receptor 84 FWD
GGTGCAGTGCAGGGAAATG	Vomeronasal 1 receptor 84 REV
GCACCATGATTCAGCTGATTCTC	Vomeronasal 2, receptor 69 FWD
TCACTGAACCTTTGTTGCAAACA	Vomeronasal 2, receptor 69 REV
ACTGGCACTAGGGAGCTTCACT	Vomeronasal 2, receptor 18 FWD
CTGCAGAACACCACCATACTGAAT	Vomeronasal 2, receptor 18 REV
AAGAAGGTGGTGAAGCAGGCATC	Gapdh FWD
CGAAGGTGGAAGAGTGGGAGTTG	Gapdh REV